Preprint Title Graphene Synthesis by Ultrasound Energy Assisted Exfoliation of Graphite in Various Solvents

Authors Betül Gürünlü, Çiğdem Taşdelen-Yücedağ and Mahmut Bayramoğlu

Publication Date 08 Okt. 2020

Article Type Full Research Paper

Supporting Information File 1 Supporting Information.docx; 2.3 MB

ORCID® iDs Betül Gürünlü - https://orcid.org/0000-0003-4437-3872; Çiğdem Taşdelen-Yücedağ - https://orcid.org/0000-0003-1232-5462; Mahmut Bayramoğlu - https://orcid.org/0000-0001-6936-1216

Full Research Paper

Graphene Synthesis by Ultrasound Energy Assisted Exfoliation of Graphite in Various Solvents

Betül Gürünlü[1,*], Çiğdem Taşdelen-Yücedağ[2,*] and Mahmut Bayramoğlu[2]

[1] Gebze Technical University, Institute of Nanotechnology, Kocaeli Turkey

[2] Gebze Technical University, Chemical Engineering Department, Kocaeli, Turkey; cigdem@ gtu.edu.tr (Ç.T.Y.); mbayramoglu@gtu.edu.tr (M.B.)

***** Correspondence: bgurunlu@gtu.edu.tr; Tel.: +90-544-354-9288 (B.G.), cigdem@gtu.edu.tr

Abstract: Liquid Phase Exfoliation (LPE) method has been gaining increasing interest by academic and industrial researchers due to its simplicity, low-cost, and scalability. High intensity ultrasound energy was exploited to transform graphite to graphene in the solvents of dimethyl sulfoxide (DMSO), N,N-dimethyl formamide (DMF), and perchloric acid (PA) without any surfactants or ionic liquids. The crystal structure, number of layers, particle size, and morphology of the synthesized graphene samples were characterized by X-ray Diffraction (XRD), Atomic Force Microscopy (AFM), Ultraviolet visible (UV–vis) spectroscopy, Dynamic Light Scattering (DLS), and Transmission Electron Microscopy (TEM). XRD and AFM analyses indicated that G-DMSO and G-DMF have few layers and G-PA has multilayers. The layer numbers of G-DMSO, G-DMF, and G-PA were determined as 9, 10, and 21, respectively. By DLS analysis, the particle sizes of graphene samples were estimated in a few micrometers. TEM analyses showed that G-DMSO and G-DMF possess sheet-like fewer layers and also, G-PA has wrinkled and unordered multilayers.

Keywords: ultrasound; liquid-phase exfoliation; graphene synthesis

---

1. Introduction

Graphene is a versatile nanomaterial with a wide range of chemical, environmental, medical, industrial, electronical applications by the means of its remarkable thermal conductivity (above

3000 W m K^{-1}); superior mechanical properties with a Young's modulus of 1 TPa, an extraordinary large specific surface area (2620 m^2 g^{-1}), and intrinsic strength of 130 GPa; and an extremely high electronic conductivity (room-temperature electron mobility of 2.5×10^5 cm^2 V^{-1} s^{-1}).[1-3]. This combination of spectacular properties enables its utilization in the production of different devices such as the electronics with high-speed and radio-frequency logic, sensors, membranes, composites with high thermal and electrical conductivity, displays with superior transparency and flexibility, solar cells, coatings, highly thin carbon films, electronic circuits, etc. [4].

Few-layered graphene has been synthesized by numerous methods including mechanical cleavage, liquid-phase exfoliation, gas-phase synthesis, Hummers' method, unrolling of multi-walled carbon nanotubes (MWCNT), chemical vapor deposition (CVD), epitaxial growth, electrochemical reaction [2,5-15]. However, these methods have some drawbacks such as low yield ratio, high-energy consumption, the use of expensive substrates as well as the difficulty of obtaining high quality product. Scientists have studied on developing more efficient synthesis methods apart from the most popular Hummers' method employing the oxidative exfoliation of natural graphite by harsh acid treatments. Final products attained by Hummers' method have many functional groups such as hydroxyls, carbonyls and carboxyls which cannot be completely removed by additional reduction and annealing treatments [16,17]. Also, the oxidation-reduction processes of Hummers' method disrupt the original honeycomb structure of graphene. This deteriorated structure reduces the electronical and the mechanical properties of the synthesized final graphene products [18-19]. For this reason, selection of the appropriate solvent and process parameters has a critical importance in order to obtain the graphene with well-arranged structure. Liquid-phase exfoliation (LPE) is one of the most feasible methods for industrial production of graphene through its scalability and low-cost. A highly stable dispersion of mono/few layered graphene products with defect-free honeycomb structure have been synthesized by LPE of graphite by applying different techniques such as shear mixing, microwave irradiation or sonication [20]. The application of the LPE method is especially significant for the electronics industry which requires graphene with defect-free and no oxide groups [21].

The LPE technique is based on the exfoliation of graphite intercalated compounds in an appropriate solvent. In this technique, there are three subsequent steps: (1) dispersion of graphite in a solvent, (2) exfoliation, and (3) purification [22]. For the intercalation of the solvent molecules, the Van der Waals forces between the graphite layers are overcome by the application of the external driving force such as ultrasound energy [23]. Then, individual layers start to slip out from the layered

structure of graphite under the effect of shear force. By this fragmentation, the thinner graphene flakes with a small lateral size can be achieved. The utilization of the ultrasound energy in various types of chemical processes relies on the acoustic cavitation in a liquid. Main elements of the acoustic cavitation are the formation, development, and collapse of cavitation bubbles. Steam bubbles emerge due to the pressure drop in some parts of liquid. On the other hand, the rise in pressure and temperature causes the extinction of the cavities. When the liquid is subjected to the ultrasound energy, localized hot points appear with high temperature and pressure.

The efficiency of the ultrasound energy is determined by the ultrasound application conditions and the type of ultrasound device. There are two types of ultrasound generators: horn-type and bath-type. Epoxy/graphene nanocomposites synthesized by using horn-type device demonstrate higher modulus and flexural strength properties than that of the samples produced via bath-type device. The reason for obtaining better properties with horn-type device is the direct immersion of the probe into the sonication liquid. This direct sonication results in the turbulent flow conditions and acoustic streaming in suspensions which prevents the agglomeration of the nanoparticles. In the case of graphene synthesis by the LPE method with ultrasonication, traditional bath type sonicator is inadequate to produce intense cavitation for the efficient exfoliation of graphite without chemicals such as ionic liquids and surfactants.

The properties of the liquid establishing the environment for the chemical processes have a great impact on obtaining the stable graphite-solvent dispersion [24]. Many studies were conducted to investigate the most convenient solvent type and optimum process conditions for the synthesis of graphene by ultrasonication [25-27]. Graphite is easily exfoliated in polar aprotic organic solvents due to its hydrophobic character. In this study, polar aprotic dimethyl sulfoxide (DMSO) and dimethyl formamide (DMF) are used for exfoliation of graphite as the sonication liquid without adding any surfactants or ionic liquids. The chemical structures of used solvents were given in Fig 1.

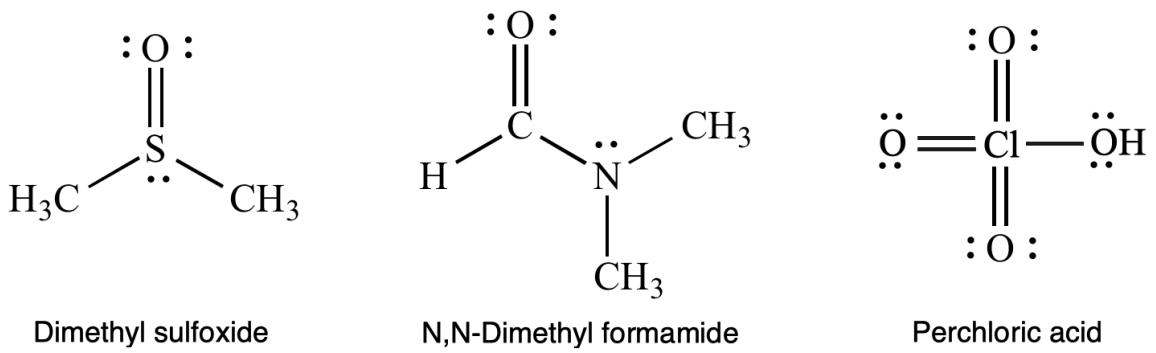

Figure 1. Lewis structure of the solvents used as liquid medium in the exfoliation of graphite.

These solvents are capable of successful exfoliation of the graphite and prevention of the graphene transformation back to graphite structure. Also, perchloric acid (PA) was chosen as the third sonication medium since it is a highly effective intercalating agent and it minimizes the defects in the honeycomb lattice of graphene at high acid concentrations of PA [28-30].

Herein, one-pot synthesis of graphene was carried out by using the horn-type ultrasound device for the exfoliation of graphite in DMSO, DMF, and PA. After the exfoliation step, the particle size, the layer number and thickness, and morphology were determined by XRD, AFM, UV-vis, DLS, and TEM analyses. Although there are some reports on the LPE of graphite, most of these methods employed organic solvents mixing them with ionic liquids and surfactant in order to obtain the stable dispersion of graphite. In this work, the effect of prolonged exposure time of intense ultrasound energy on graphene properties was investigated by applying LPE technique in organic solvents without adding any ionic liquids or surfactant.

2. Experimental

2.1. Materials

Graphite fine powder (Extra pure) and commercial graphene (CG) were purchased from, Asbury Inc., New Jersey, and XG Sciences, Michigan, US, respectively. Dimethyl sulfoxide - DMSO (Merck), N,N-dimethylformamide – DMF (Merck), perchloric acid 70-72% - PA (Merck) were of analytical grade and used as received. CG was used as control sample in order to compare the precision and purity of the synthesized graphene products.

2.2. Method

0.3 g graphite was dispersed in a 50 mL solvent such as DMSO, DMF and PA. The prepared dispersions were sonicated for 3 hours by using BANDELIN® HD 2200 SONOPULS equipped with a VS 190 T sonotrode made of titanium alloy, 200 W, 50 % amplitude (Fig. 2). Afterwards, these dispersions were subjected to Elektromag, M 4812 P for an hour at 3000 rpm in order to remove the unexfoliated graphite particles. Then, the large aggregates were settled down, supernatant part of the samples were decanted and collected in separate vials.

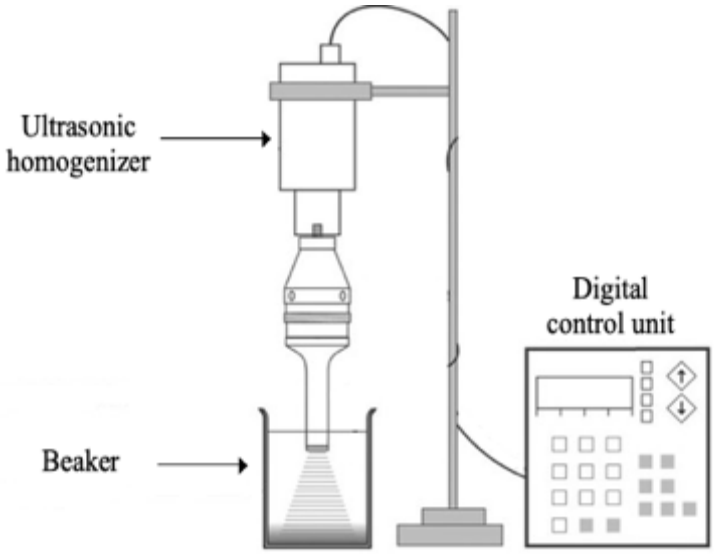

Figure 2. Ultrasonic treatment unit.

2.3 Characterization

X-ray diffraction (XRD) was conducted by depositing the samples onto glass pieces (0.7 x 0.7 mm^2) and their XRD spectra were determined by a Rigaku D-Max 2200 Series device equipped with Cu-Kα radiation (λ = 1.54 Å) at a scanning rate of 3°per minute. Its tube voltage was 40 kV and the current was 40 mA. Samples for AFM were prepared by dropping the graphene dispersions onto glass pieces (0.7 x 0.7 mm^2) and measurements were carried out in contact (tapping) mode, with 10.00 μm scan size, and 20.35 Hz scan rate by using Digital Instruments Nanoscope. Ultraviolet-visible (UV-vis) spectroscopy analyses were done by a Perkin Elmer Precisely Lambda 35 UV-vis Spectrometer in the region from 200 to 800 nm. In order to elucidate the mechanical properties, the particle size distribution analyses were carried out by dynamic light scattering (DLS) method through Malvern Zetasizer Nano ZS Laser particle size distribution meter. The structural and morphological properties were determined by the measurements made by a Hitachi HT7800 model transmission electron microscope (TEM) that is operating at 120 kV.

3. Results & Discussion

In this study, ultrasound assisted exfoliation of graphite was conducted in DMSO, DMF, and PA solvents (Fig. 3). The synthesized graphene products are characterized by comparing the properties with that of CG. First of all, graphite was added into the solvent, then the mixture was exposed to ultrasound energy generated by a horn-type device. This type of sonicators produce high-intensity ultrasound energy which enables the stable micromechanical exfoliation of graphite. The inverse segregation and micelle cumulation of graphenes were avoided by the utilization of high-intensity ultrasound energy particularly in solvents such as DMSO, DMF, ethylene glycol or their aqueous solutions [31]. Additionally, horn-type sonicator provides the synthesis of graphene with minor functional groups and graphene having flat and defect free morphologies.

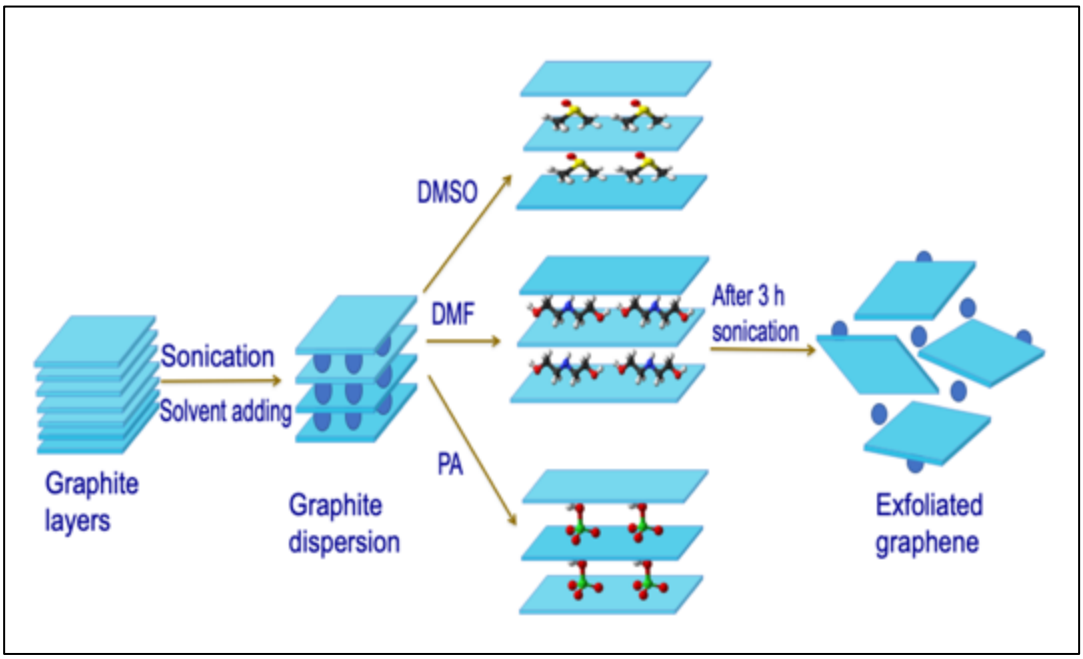

Figure 3. The exfoliation mechanism of the graphite to graphene.

The stable homogeneous dispersion of graphite can be achieved in solvents such as DMSO, DMF, and PA possessing similar surface tensions close to that of graphene (~68 mJ/m^2) [32,33]. The surface energies of DMSO, DMF, and PA are 43.54, 37.1, and 70 mJ/m^2, respectively. When the surface energies of dispersed phase and dispersant are close to each other, the enthalpy of mixing is diminished resulting in a stable dispersion of graphite. The crystal structure and the layer numbers of the graphene products (G-DMSO, G-DMF and G-PA) were determined by XRD analysis given in Fig. 4. It is well-known that the peak at 2θ° = 26.5 indicates the graphene characteristic structure.

According to the XRD spectra, decline in the intensity of this peak demonstrated the transformation of graphite to graphene [34].

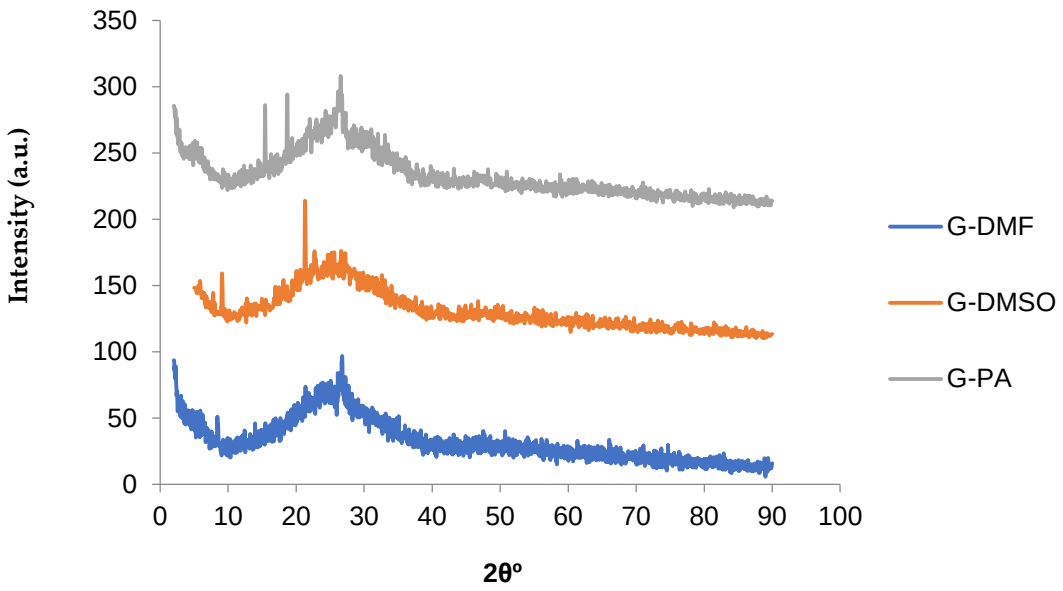

Figure 4. XRD results of synthesized graphene products.

The thickness of graphene products was estimated by applying Scherrer's equation which is stated as $D_{002} = K\lambda/B\cos\theta$. D_{002}, K, λ, B, and θ are the thickness of the graphene, a constant based on the crystal shape (0.89), the wavelength of the X-ray (0.15406 nm), the full width half maximum (FWHM) of the characteristic peak of graphene, and the scattering angle, respectively [35,36]. The number of layers was calculated by the following equation: $N_{GP} = D_{002}/d_{002}$, where d_{002} is the interlayer distance [37,38]. The calculated layer numbers of G-DMSO, G-DMF, and G-PA are 9, 10, and 20, respectively. Although the layer numbers of G-DMSO and G-DMF were very close to each other, G-PA gave a higher layer number. This higher layer number value may be explained by the inverse segregation of graphene particles synthesized in PA.

The thickness and surface roughness values of G-DMSO, G-DMF, and G-PA are determined via AFM analysis given in Fig. 5. Roughness average (Ra) is defined as the arithmetic mean of the absolute values of the height alterations from the mean line along the profile. The square root of the arithmetic mean surface roughness (Rq) is also described to take into account the big peaks and valleys [39]. Additionally, the roughness mean square (RMS) is calculated by using height values of microscopic peaks and valleys. As seen from Fig. 5, the Ra values are 2.937, 6.343, and 15.453 nm,

whereas the Rq values are 3.471, 8.046, and 17.258 nm for G-DMSO, G-DMF, and G-PA, respectively. Furthermore, the RMS values are determined as 5.675, 8.842, and 19.291 nm for G-DMSO, G-DMF, and G-PA, respectively.

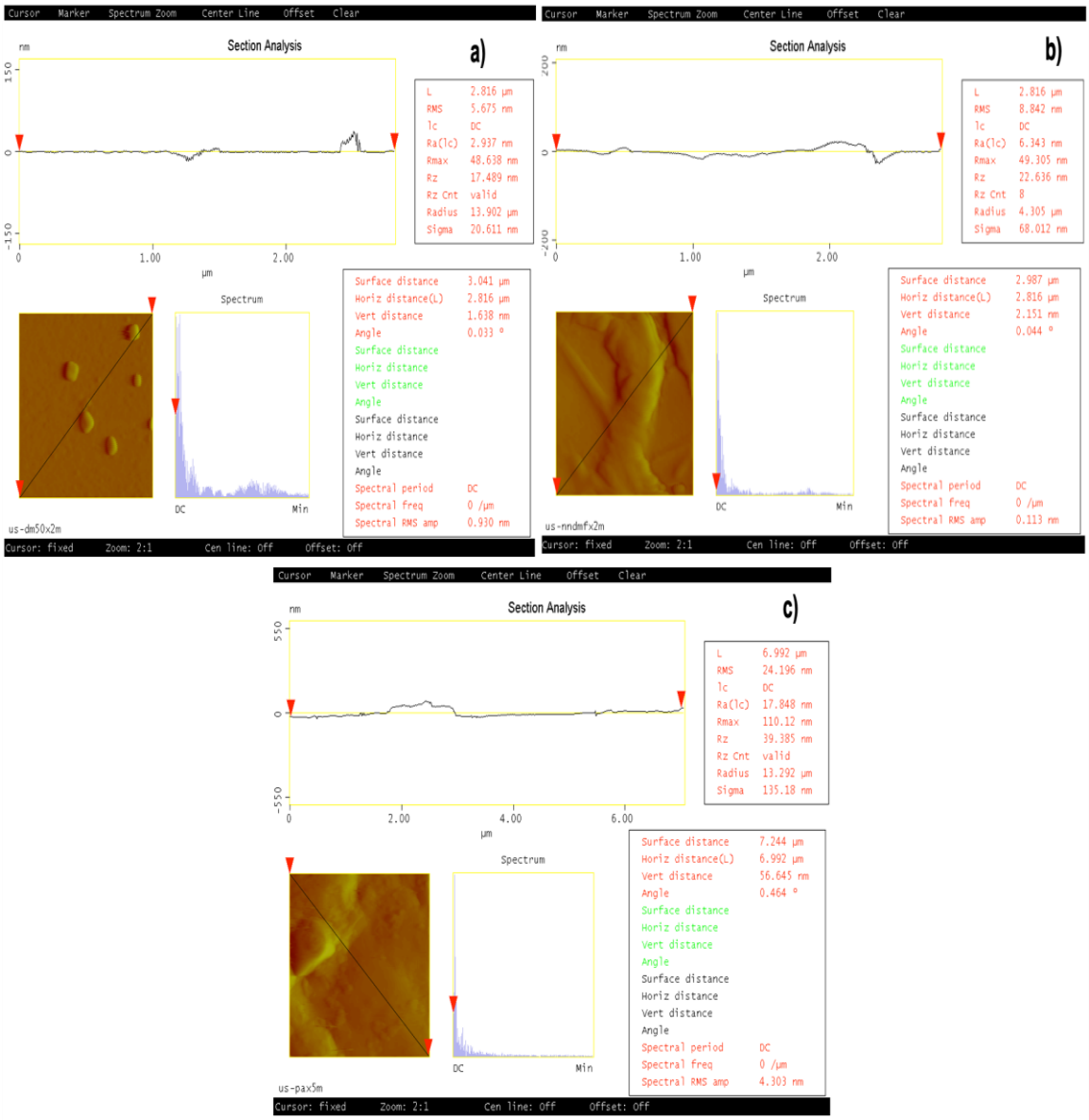

Figure 5. The AFM images of a) G-DMSO, b) G-DMF, and c) G-PA drop casted onto glass piece showing the homogeneous structure of the pristine graphene nanosheets.

In order to confirm the number of graphene layers, AFM results were exploited as well. The following equation was used for the calculation of layer numbers: $N = (t_{measured}-0.4)/0.335$, where $t_{measured}$ is the vertical distance. The value of 0.335 nm is the thickness of the single layer graphene (SLG). Since the mica was used as substrate material in AFM measurements, the height was

accepted as 0.4 nm [40]. The thickness ($t_{measured}$) values of the graphene samples were measured as 1.638, 2.151, and 7.284 nm for G-DMSO, G-DMF, and G-PA, respectively. The number of layers were calculated from the aforementioned equation as 3.69 ≅ 4, 5.22 ≅ 5, and 21.053 ≅ 21 for G-DMSO, G-DMF, and G-PA, respectively. When all the results were assessed, the roughness and the layer number values of G-DMSO and G-DMF are smaller than that of G-PA. The layer numbers of graphene products obtained from XRD agree with those estimated from the AFM. It can be inferred from these findings while G-DMSO and G-DMF include fewer layers, G-PA has multi layered structure. In the case of preparation of graphene in PA, the RMS and layer number are 19.291 nm and 21, respectively. For the sample of G-DMSO, RMS and layer number are 5.675 nm and 4, respectively. The multilayered specimen of G-PA has a higher RMS value which is in accordance with literature [41]. It is believed that the combined effect of high-power ultrasound energy and strong acidity of PA might trigger the formation of some functionalities on the graphene leading to an increase in the surface roughness. Also, the reason for higher thickness may be due to the out of plane rippling behaviour of graphene [42]. In order to clarify the graphene structure, UV-vis spectra of the graphene dispersions were recorded as seen in Fig. 6. The graphene samples, which are labeled as G-DMSO, G-DMF and G-PA, showed peak at 265 nm wavelength referring to sp^2 C=C bonds [43].

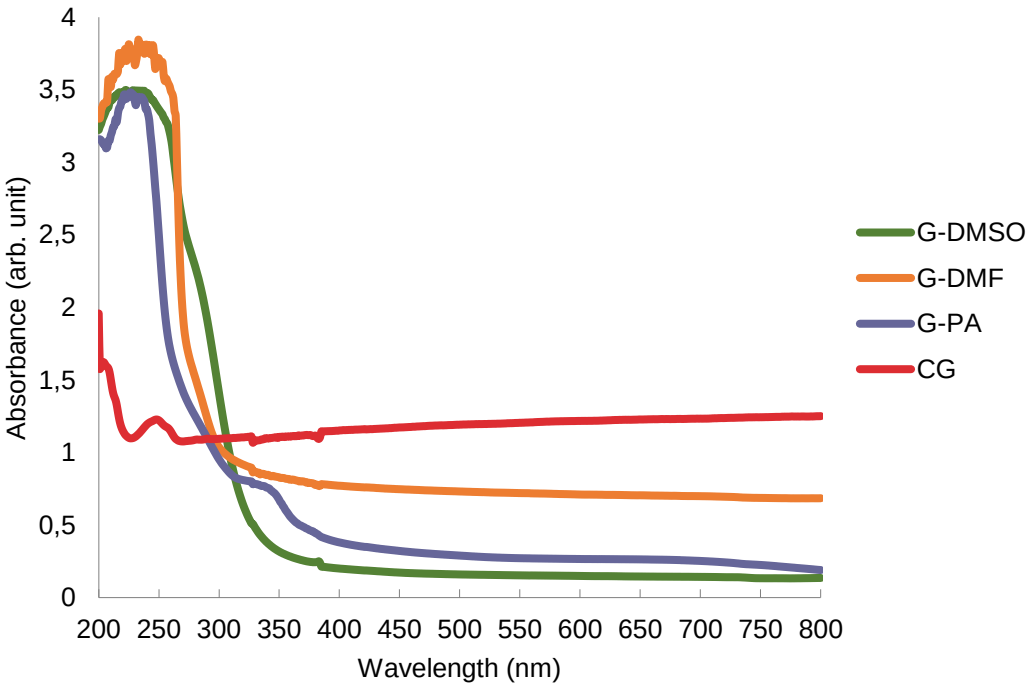

Figure 6. UV-vis spectra of CG, G-DMSO, G-DMF, and G-PA products.

Next, dynamic light scattering (DLS) technique, which gives the apparent size of the graphene samples in the aqueous dispersion, was applied to investigate the particle size [44]. The size distribution results are presented in Fig. 7.

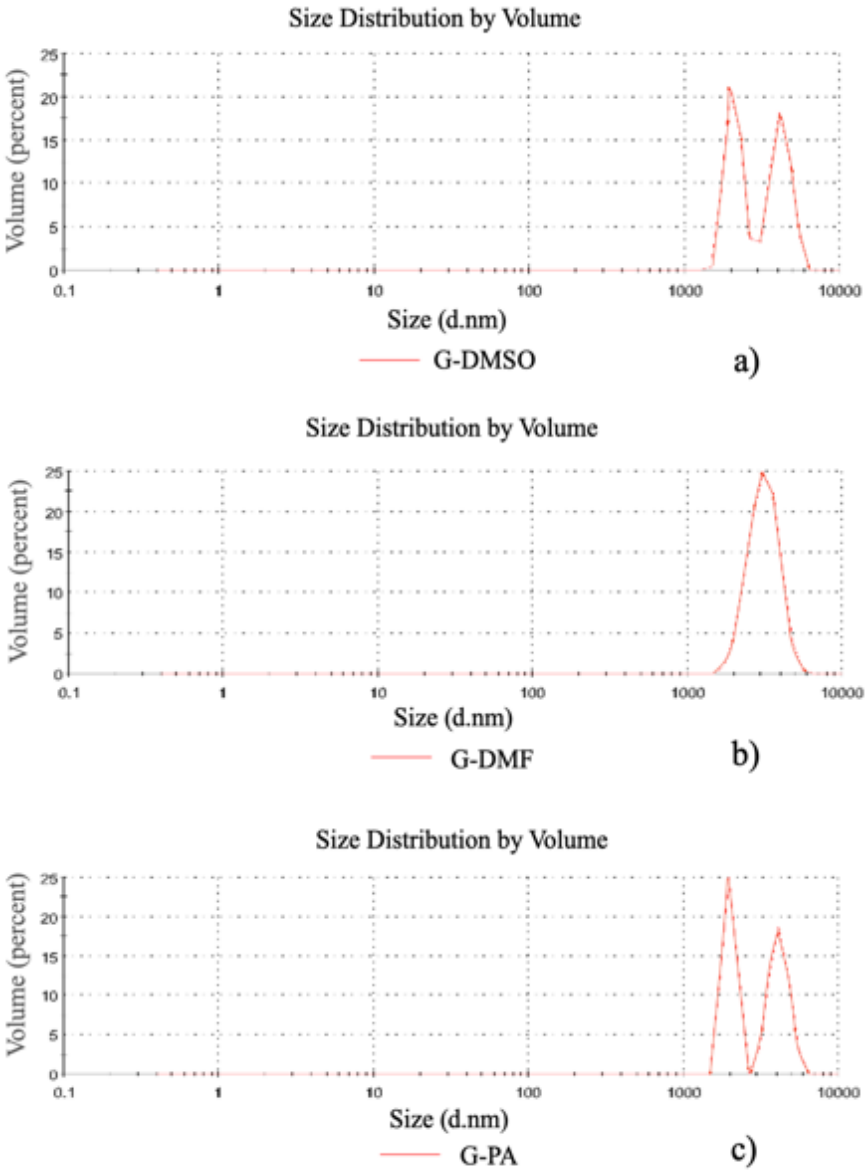

Figure 7. Particle size analysis results of synthesized samples, a) G-DMSO, b) G-DMF, c) G-PA.

As seen in Table 1, Z-average hydrodynamic radius (Rh) values of G-DMSO, G-DMF and G-PA are 6938, 3846 and 7137 nm, respectively. These results are parallel to the previous studies which reported that graphene samples with a few micrometers of Rh had less defected structure. The

graphenes with this particle size are promising and favourable for the applications in electronics industry [27,45].

Table 1. Particle size results of synthesized samples

Sample Name	Z-Ave (d.nm)	Std. Dev. (d.nm)
G-DMF	3846	706.7
G-DMSO	6938	408
G-PA	7137	207.5

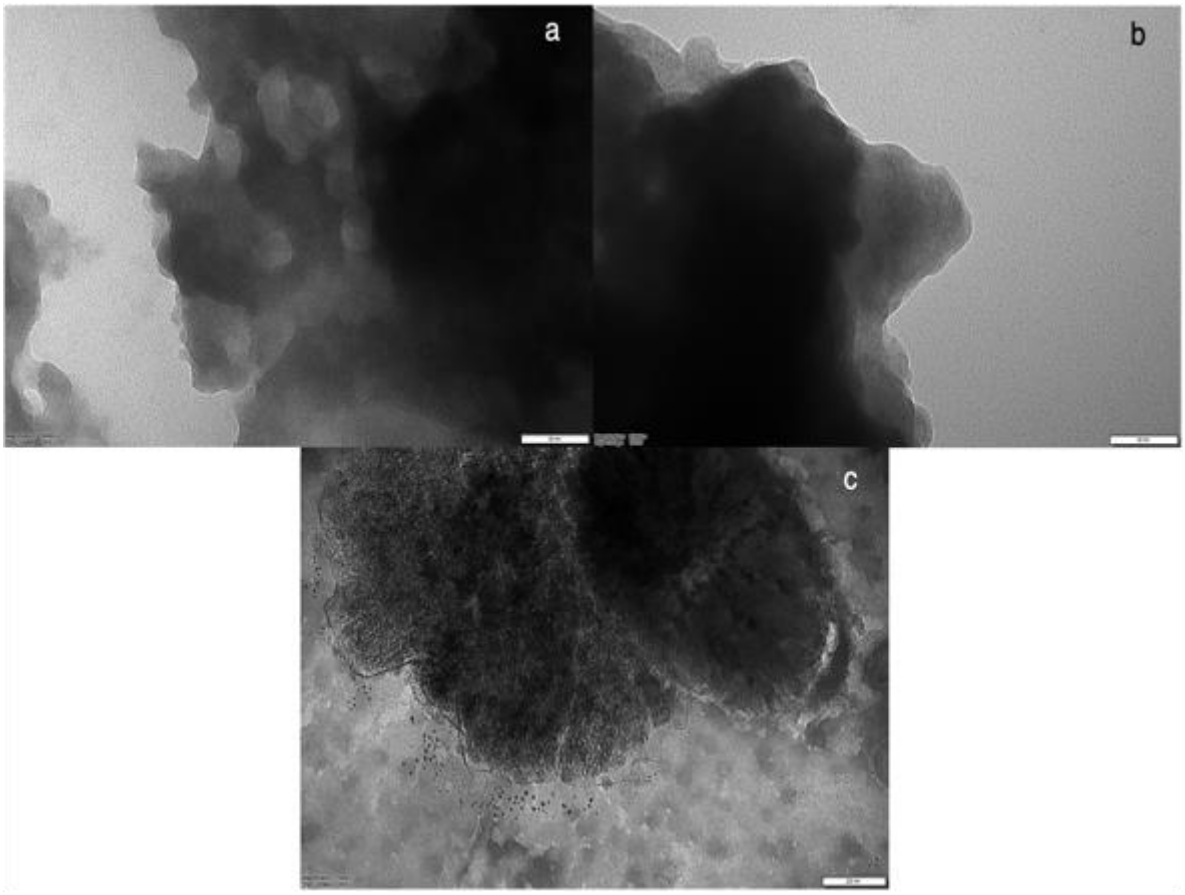

Figure 8. TEM images of graphene layers in sample a) G-DMSO, b) G-DMF d) G-PA. Scale bar: a) 50 nm, b) 50 nm, and c) 200 nm.

Fig. 8 illustrates the TEM images of graphene products of G-DMSO, G-DMF, and G-PA. TEM analysis revealed that G-DMSO and G-DMF have fewer layers while G-PA has multilayers. The light and dark coloured parts (Fig. 7a and 7b) represent the few layered structures at the edges of the sample and the multilayered agglomerates at the surface, respectively. Also, Fig. 7a and 7b exhibit

the sheet-like flakes of graphene structure overlapping at some parts. Fig. 7c presents a wrinkled and unordered structure of G-PA, which was synthesized by excessive cavitation in PA. Due to the high acidic character of PA, crumbled structure and deficiencies, low quality properties were observed on the surface morphology of the sample. Moreover, the dark coloured parts on the image of G-PA display the contamination arising from the residual solvent [46].

4. Conclusion

In summary, ultrasound assisted LPE method was used for the synthesis of graphene in the solvents of DMSO, DMF, and PA. According to XRD results, the layer numbers of the samples labelled as G-DMSO, G-DMF, and G-PA were estimated as 9, 10, and 20, respectively. The UV-vis spectra of all the samples give peak at 265 nm wavelengths indicating the sp^2 C=C bonds of graphene. Also, the results of AFM showed that the layer numbers are 4, 5, and 21 whereas Z-average hydrodynamic radius (Rh) are 6930, 3846 and 7137 nm for G-DMSO, G-DMF, and G-PA, respectively.

XRD, AFM, and TEM revealed that G-DMSO and G-DMF contain few layers while G-PA has multilayer structure. Finally, it can be concluded that DMSO is a promising solvent for the one-pot synthesis of few-layered graphene by LPE method without using any surfactants or ionic liquids.

Author Contributions: Conceptualization, B.G., Ç.T.Y. and M.B.; methodology, B.G., Ç.T.Y. and M.B.; software, B.G., Ç.T.Y. and M.B.; validation, B.G., Ç.T.Y. and M.B.; formal analysis, B.G., Ç.T.Y. and M.B..; investigation, B.G., Ç.T.Y. and M.B.; resources, B.G., Ç.T.Y. and M.B.; data curation, B.G., Ç.T.Y. and M.B.; writing—original draft preparation, B.G., Ç.T.Y. and M.B.; writing—review and editing, B.G., Ç.T.Y. and M.B.; visualization, B.G., Ç.T.Y. and M.B.; supervision, B.G., Ç.T.Y. and M.B.; project administration, B.G., Ç.T.Y. and M.B..; funding acquisition, B.G., Ç.T.Y. and M.B. All authors have read and agreed to the published version of the manuscript.

Funding: This work has been partially supported by Research Fund of the Gebze Technical University (project no. 2018-A105-55)

Acknowledgments: This work has been partially supported by Research Fund of the Gebze Technical University (project no. 2018-A105-55). The authors also acknowledge the Materials Science and Engineering Department of Gebze Technical University for providing AFM and DLS measurements.

Conflicts of Interest: The authors declare no conflict of interest.

References

1. Geim, A.K.; Novoselov, K.S. The rise of graphene. *Nat. Mater.* **2007**, *6*, 183-191.
2. Novoselov, K.S.; Geim, A.K.; Morozov, S.V.; Jiang, D.; Zhang, Y.; Dubonos, S.V.; Grigorieva, I.V.; Firsov, A.A. Electric field effect in atomically thin carbon films. *Science* **2004**, *306*, 666-669.
3. Georgakilas, V.; Otyepka, M.; Bourlinos, A.B.; Chandra, V.; Kim, N.; Kemp, K.C.; Hobza, P.; Zboril, R.; Kim, K.S. Functionalization of graphene: covalent and non-covalent approaches, derivatives and applications. *Chem. Rev.* **2012**, *112*, 6156-6214.
4. Allen, M.J.; Tung, V.C., Kaner, R.B. Honeycomb Carbon: A Review of Graphene. *Chem. Rev.* **2010**, *110*, 132-145.
5. Zhang, X.; Coleman, A.C.; Katsonis, N.; Browne, W.R.; Wees, B. J. van; Feringa, B.L. Dispersion of Graphene in Ethanol Using a Simple Solvent Exchange Method. *Chem. Commun.* **2010**, *46*, 7539-7541.
6. Stankovich, S.; Dikin, D.A.; Piner, R. D.; Kohlhaas, K. A.; Kleinhammes, A.; Jia, Y.; Wu, Y.; Nguyen, S.T.; Ruoff, R. S. Synthesis of graphene-based nanosheets via chemical reduction of exfoliated graphite oxide. *Carbon* **2007**, *45*, 1558-1565.
7. Compton, O.C.; Nguyen, S.B.T. Graphene Oxide, Highly Reduced Graphene Oxide, and Graphene: Versatile Building Blocks for Carbon-Based Materials. *Small* **2010**, *6*, 711-723.
8. Qi, X.; Pu, K.-Y.; Zhou, X.; Li, H.; Liu, B.; Boey, F.; Huang, W.; Zhang, H. Conjugated-Polyelectrolyte-Functionalized Reduced Graphene Oxide with Excellent Solubility and Stability in Polar Solvents. *Small* **2010**, *21(6)*, 663-669.
9. Vadahanambi, S.; Jung, J.-H.; Kumar, R.; Kim, H.-J.; Oh, I.-K. An ionic liquid-assisted method for splitting carbon nanotubes to produce graphene nano-ribbons by microwave radiation. *Carbon* **2013**, *53*, 391-398.
10. Kleinschmidt, A.C.; Donato, R.K.; Perchacz, M.; Benes, H.; Stengl, V.; Amico, S.C.; Schrekker, H.S. “Unrolling” multi-walled carbon nanotubes with ionic liquids: application as fillers in epoxy-based nanocomposites. *RSC Adv.* **2014**, *4*, 43436.
11. Liu, Q., Fujigaya, T.; Nakashima, N. Graphene unrolled from ‘cup-stacked’ carbon nanotubes. *Carbon* **2012**, *50*, 5421-5428.
12. Emtsey, K.V.; Bostwick, A.; Horn, K.; Jobst, J.; Kellogg, G.L.; Ley, L.; McChesney, J.L.; Ohta, T.; Reshanov, S.A., Rohrl, J.; Rotenberg, E; Schmid; A.K.; Waldmann, D.; Weber, H.B.; Seyller, T. Towards Wafer-Size Graphene Layers by Atmospheric Pressure Graphitization of Silicon Carbide. *Nat. Mater.* **2009**, *8*, 203-207.

13. Li, X.; Cai, W.; An, J.; Kim, S.; Nah, J.; Yang, D.; Piner, R.; Velamakanni, A.; Jung, I.; Tutuc, E.; Banerjee, S. K.; Colombo, L.; Ruoff, R.S. Large-area Synthesis of High-Quality and Uniform Graphene Films on Copper Foils. *Science* **2009**, *324*, 1312-1314.
14. Lee, J.-W.; Kim, M.; Na, W.; Hong, S.M.; Koo, C.M. Fabrication of high quality graphene nanosheets via a spontaneous electrochemical reaction process. *Carbon* **2015**, *91*, 527-534.
15. Dato, A.; Radmilovic, V.; Lee, Z.; Phillips, J.; Frenklach, M. Substrate-free Gas-Phase Synthesis of Graphene Sheets. *Nano Lett.* **2008**, *8*, 2012-2016.
16. Li, X.; Zhang, G.; Bai, X.; Sun, X.; Wang, X.; Wang, E.; Dai, H. Highly conducting graphene sheets and Langmuir–Blodgett films, *Nat. Nanotechnol.* **2008**, *3*, 538–542.
17. Stankovich, S.; Dikin, D.A.; Piner, R.D.; Kohlhaas, K.A.; Kleinhammes, A.; Jia, Y.; Wu, Y.; Nguyen, S.T.; Ruoff, R.S. Synthesis of graphene-based nanosheets via chemical reduction of exfoliated graphite oxide, *Carbon* **2007**, *45*, 1558–1565.
18. Guo, S.; Dong, S. Graphene nanosheet: synthesis, molecular engineering, thin film, hybrids, and energy and analytical applications. *Chem. Soc. Rev*. **2011**, *40*, 2644-2672.
19. Rao, C.N.R.; Sood, A.K.; Subrahmanyam, K.S.; Govindaraj, A. Graphene: The New Two-Dimensional Nanomaterial. *Angew. Chem. Int*, *Ed.*, **2009**, *48*, 7752-7777.
20. Lotya, M.; King, P. J.; Khan, U.; De, S.; Coleman, J. N. High-Concentration, Surfactant-Stabilized Graphene Dispersions. *ACS Nano*, **2010**, *4*, 3155−3162.
21. Lotya, M.; Hernandez, Y.; King, P. J.; Smith, R. J.; Nicolosi, V.; Karlsson, L. S.; Blighe, F. M.; De, S.; Wang, Z. M.; McGovern, I. T.; et al. Liquid Phase Production of Graphene by Exfoliation of Graphite in Surfactant/Water Solutions. *J. Am. Chem. Soc*. **2009**, *131*, 3611−3620.
22. Ciesielski, A.; and Samori, P. Graphene via sonication assisted liquid-phase exfoliation. *Chem. Soc. Rev.* **2014**, *43*, 381- 398.
23. Xu, H.; Zeiger, B. W.; and Suslick, K. S. Sonochemical synthesis of nanomaterials *Chem. Soc. Rev.* **2013**, *42(7)*, 2555-2567.
24. Whitener, K. E., Jr; Sheehan, P. E. Graphene synthesis. *Diamond Relat. Mate*r. **2014**, *46*, 25−34.
25. Yi, M.; Shen, Z. A review on mechanical exfoliation for the scalable production of graphene. *J. Mater. Chem. A* **2015**, *3*, 11700−11715.
26. Blake, P.; Brimicombe, P. D.; Nair, R. R.; Booth, T. J.; Jiang, D.; Schedin, F.; Ponomarenko, L. A.; Morozov, S. V.; Gleeson, H. F.; Hill, E. W.; Geim, A. K.; Novoselov, K. S. Graphene-based liquid crystal device. *Nano Lett.* **2008**, *8*, 1704−1708.
27. Hernandez, Y.; Nicolosi, V.; Lotya, M.; Blighe, F. M.; Sun, Z.; De, S.; McGovern, I. T.; Holland, B.; Byrne, M.; Gun'ko, Y. K.; Boland, J. J.; Niraj, P.; Duesberg, G.; Krishnamurthy, S.; Goodhue, R.; Hutchison, J.; Scardaci, V.; Ferrari, A. C.; Coleman, J. N. High-yield production of graphene by liquid-phase exfoliation of graphite. *Nat. Nanotechnol.* **2008**, *3*, 563−568.

28. Schnyder, B.; Alliata, D.; Kötz, R.; Siegenthaler, H. Electrochemical intercalation of perchlorate ions in HOPG: an SFM/LFM and XPS study. *Appl Surf Sci* **2001**, *173(3–4)*, 221-232.
29. Beck, F.; Junge, H.; Krohn, H. Graphite intercalation compounds as positive electrodes in galvanic cells. *Electrochim Acta* **1981**, *26(7)*, 799-809.
30. Zhang, J.; and Wang, E. STM investigation of HOPG superperiodic features caused by electrochemical pretreatment. *J Electroanal Chem* **1995**, 399(1–2), 83-89.
31. Štengl, V., Preparation of graphene by Using an Intense Cavitation Field in a Pressurized Ultrasonic Reactor. *Chem Eur. J.* **2012**, *18*,14047-14054.
32. Coleman, J.N. Liquid Exfoliation of Defect-Free Graphene. *Acc. Chem. Res.* **2013**, *46*, 14-22.
33. Wang, S.; Zhang, Y.; Abidi, N.; Cabrales, L. Wettability and Surface Free Energy of Graphene Films. *Langmuir*, **2009**, *25*, 11078-11081.
34. Simón, M.; Benítez, A.; Caballero, A.; Morales, J.; Vargas, O. Untreated Natural Graphite as a Graphene Source for High-Performance Li-Ion Batteries. *Batteries* **2018**, *4(1)*, 13.
35. Su, F.; Zhao, X.S.; Wang, Y.; Wang, L.; and J. Y. Lee, Hollow carbon spheres with a controllable shell structure. *Journal of Materials Chemistry* **2006**, *16(45)*, 4413–4419.
36. Adel, M.; el-Maghraby, A.; el-Shazly, O.; el-Wahidy, E.W.F.; and Mohamed, M.A.A. Synthesis of few-layer graphene-like nanosheets from glucose: new facile approach for graphene-like nanosheets large-scale production. *Journal of Materials Research*, **2016**, *31(4)*, 455–467.
37. Ju, H.M.; Huh, S.H.; Choi, S.H.; and Lee, H.L. Structures of thermally and chemically reduced graphene. *Materials Letters*, **2010**, *64(3)*, 357–360.
38. Uran, S.; Alhani, A.; and Silva, C. Study of ultraviolet-visible light absorbance of exfoliated graphite forms. *AIP Advances*, **2017**, *7(3)*, article 035323.
39. Bhushan, B. Modern Tribology Handbook, Two Volume Set, 1st Edition, 2001, Boca Raton, CRC Press.
40. Gürünlü, B.; Taşdelen-Yücedağ, Ç.; and Bayramoğlu, M. R. Green Synthesis of Graphene from Graphite in Molten Salt Medium. *Journal of Nanomaterials*, **2020**, *2020*, 7029601.
41. Kim, H. J.; Penkov, O. V.; and Kim, D. E. Tribological properties of graphene oxide nanosheet coating fabricated by using electrodynamic spraying process. *Tribology Letters* **2015**, *57(3)*, 11249-015-0467-8.

42. Zhou, L.; Fox, L.; Włodek, M.; Islas, L.; Slastanova, A.; Robles, E.; Bikondoa, O.; Harniman, R.; Fox, N.; Cattelan, M.; and Briscoe, W. H. Surface structure of few layer graphene, *Carbon* **2018**, *136*, 255-261.

43. Johra, F. T.; Lee, J. W.; and Jung, W. G. Facile and safe graphene preparation on solution-based platform. *Journal of Industrial and Engineering Chemistry* **2014**; *20(5)*, 2883-2887.

44. Lotya, M.; Rakovich, A.; Donegan, J.F.; Coleman, J.N. Measuring the lateral size of liquid-exfoliated nanosheets with dynamic light scattering. *Nanotechnology* **2013**, *24*, 265703.

45. Green, A. A.; Hersam, M. C. Emerging Methods for Producing Monodisperse Graphene Dispersions. *J. Phys. Chem. Lett.* **2010**, *1(2)*, 544-549.

46. Güler, Ö.; Güler, S. H.; Selen, V.; Albayrak, M. G.; Evin, E. Production of graphene layer by liquid-phase exfoliation with low sonication power and sonication time from synthesized expanded graphite. *Fullerenes, Nanotubes and Carbon Nanostructures* **2016**, *24(2)*, 123-127.